

## QUASI SELF-COMPLEMENTARY UWB NOTCHED MICROSTRIP ANTENNA FOR USB APPLICATION

Anwer S. Abd El-Hameed<sup>1</sup>, Deena A. Salem<sup>1, \*</sup>,  
Esmat A. Abdallah<sup>1</sup>, and Essam A. Hashish<sup>2</sup>

<sup>1</sup>Electronics Research Institute, Cairo, Egypt

<sup>2</sup>Faculty of Engineering, Cairo University, Cairo, Egypt

**Abstract**—UWB antenna is a crucial part of any UWB system required for indoor application. In this paper, a novel design is presented, which relies on self-complementary structure. The structure is fed by a microstrip line, where a triangular notch is embedded in the ground plane. The design in this paper yields a UWB bandwidth that extends from 2.86.0–40.0 GHz. To ensure coexistence of UWB with WLAN applications (5.15–5.825 GHz) with minimal interference, a frequency notch is introduced using two parasitic U-shaped elements embracing the microstrip feeding line that resonates in the vicinity of the band notch frequency band. The proposed design was subject to parametric study to reach optimum parameters. The final design was fabricated using photolithographic technique and the measured results showed very good agreement with simulated ones.

### 1. INTRODUCTION

As the need for the multi-media communications is increasing rapidly, USB system using Ultra Wide Band (UWB) technique is introduced. USB specifications based on the ultra-wideband (UWB) radio gain great popularity by the multiband OFDM alliance and WiMedia alliance, which are the associations that promote personal area range wireless connectivity and interoperability among multimedia devices in a networked environment. This may be attributed to the fact that USB permits data transfer rate of 480 Mbps, when the device is within 3 m of the computer. Beyond 3 m but within 10 m, the data transfer rate is reduced to 110 Mbps. However, it is anticipated that USB

---

*Received 8 April 2013, Accepted 16 October 2013, Scheduled 31 October 2013*

\* Corresponding author: Deena A. Salem (deenasalem3@ieee.org).

speed will be able to reach 1 Gbps in the near future. As the antenna is integrated into the wireless USB in an indoor environment, it is important to know the effect of packaging on the performance of the designed antenna, and/even try to modify the prototype to mitigate any not required effects.

Self-complementary antennas (SCA's) are generally characterized by constant impedance. They are classified into two types namely, revolutionarily symmetrical shape and axially symmetrical shape. A planar metallic antenna is said to be self-complementary when the metal area and the open area are congruent. In a strict sense, self-complementarity is only defined on infinite size antennas. The self-complementary antenna is well known for its extremely broadband characteristics. As a matter of fact, the idea of the self-complementary antenna was obtained in the process of the developmental studies for the Yagi-Uda antenna [1], by Mushiake [2–4]. The impedance of the load is the characteristic impedance  $Z_o/2$  ( $= 60 \Omega$ ), where  $Z_o$  is the free space intrinsic impedance. For structures such as rotationally symmetric four-terminal self-complementary planar antenna, the input impedance of which is  $30\sqrt{2\pi}$  [6–8]. Two and three dimensional multi-planar axially symmetric two-terminal unbalance self-complementary antenna is also presented in [5, 8].

Ref. [9] presented a compact ultra-wideband self-complementary antenna (SCA) optimized for bandwidth constrained by size using Finite Difference Time Domain (FDTD) technique to analyze the complex antenna structures. The design of self-complementary antennas with pre-fractal profiles is investigated, [10] for its potentiality in designing wideband antennas. This new family of antennas was expected to combine the performances of self-complementary antennas and pre-fractals. Two new antenna designs, the self-complementary Koch-tie dipole and the Gosper Island dipole, were fully described [10]. A broadband printed self-complementary axe shape structure, have been reported to achieve 101.3%  $-10$  dB bandwidth, with good radiation performance [11]. A printed spiral antenna with a self-complementary configuration was developed in [12], which consists of spiral shaped metal strips and slots provided on ground planes as their counterparts. For balanced and unbalanced feeds, two types of antenna configurations such as single and twin spirals were fabricated and their performances were investigated. A printed ultra-wideband (UWB) antenna operating within a frequency range of 3.1–5 GHz was proposed for wireless USB dongle applications [13]. Ref. [14] presented a very simple antenna system which is composed of a monopole and a slot as its complementary element. Ref. [15] presented a printed quasi-self-complementary antenna fed by a  $50 \Omega$  microstrip line. The antenna is

composed of a quarter-circular disc and a counterpart quarter-circular slot on the ground plane for ultra-wideband applications. Furthermore, with an inverted L-shaped slit embedded on the quarter-circular disc, good performance of band-rejection capability is achieved. This allows relaxation of filtering spectrum in the radio frequency front-end.

Later, Ref. [16] modified the design in [15] as the desired band-notched (at 5.2/5.8 GHz) UWB operation which can be obtained by choosing the size of a parasitic arc-shaped strip at the backside of the quarter-circular patch. The proposed antenna in [16] has advantages of low cost, easy design and compact size. Refs. [17, 18] developed a small UWB antenna whose size is the same as the general USB stick memory size, using the triangular elements. This antenna is made of the printed circuit board without the wide ground plane, thus, covering the wide band width from 3.1 GHz to 4.9 GHz. In spite of all the impressive prospects promised by SCAs, the need of a matching network to transform the input impedance from 188.5 to  $50 \Omega$ , in order to integrate with the RF front end, adds complications to the design. In 2008, Refs. [19, 20] developed a novel and simple design of a quasi-self-complementary antenna for ultra-wideband applications. The proposed antenna, fed by a  $50 \Omega$  coplanar waveguide without using matching circuit, has a compact size, only  $0.22\lambda$  at 1.3 GHz, which is the lower end of the bandwidth.

In this paper, a new design of microstrip line-fed quasiself-complementary UWB notched (QSCA) is developed to achieve an ultra-wide impedance bandwidth, from 2.86 to 40 GHz with frequency notch at 5.5 GHz. Our design has larger bandwidth than the last mentioned designs. It also features both physically and electrically small dimensions,  $16 \text{ mm} \times 25 \text{ mm}$ . Compared with widely used UWB monopole antennas, this antenna design provides a fairly small size and reasonable radiation pattern. The basic idea of this design is that the effective side of the truncated structure would be large due to the longer path followed by the signal along the antenna borders, and the field radiated at the corners will greatly reduce the amount of energy that reflects at the truncation of the structure. Besides, if the self-complementary of the structure is maintained, the result will be a frequency independent behavior of the input impedance starting at a lower frequency.

Organization of the rest of the paper is as follows. Section 2 gives antenna design. Section 3 presents the simulation and the experimental results, while Section 4 introduces packaging effect for only a frequency range up to 20 GHz due to memory limitation. Conclusions are given in Section 5.

## 2. ANTENNA DESIGN

In this section, the design of the proposed antenna of dimension  $L \times W$  is presented. Figure 1 shows the geometry and dimensions of the proposed QSCA. The antenna is printed on FR4 substrate with thickness  $h = 1.5$  mm, relative permittivity of 4.5, and  $\tan \delta = 0.25$ . The antenna is composed of quasi self-complementary stepped triangle fed by a  $50 \Omega$  line of width  $W_f$  and linearly tapered to width  $W_t$  at the line of connection with the patch, and a triangular slot is etched from the ground plane to improve impedance matching. The feeding line is bent to connect the connector at the middle point of the long side of the component to minimize the protrusion of the USB [21–23]. The corner of the bent feeding line is chamfered at  $45^\circ$ . A slot congruent to the stepped triangle is etched in the ground plane but rotated around the vertical axis of the antenna. The prototype was designed in two stages. The first stage is concerned with the extension of the bandwidth from 2.86 GHz to 40 GHz, and the second stage is concerned with notching out WLAN frequency band 5.15–5.825-GHz. The two stages are described, and their results are presented in the following sections.

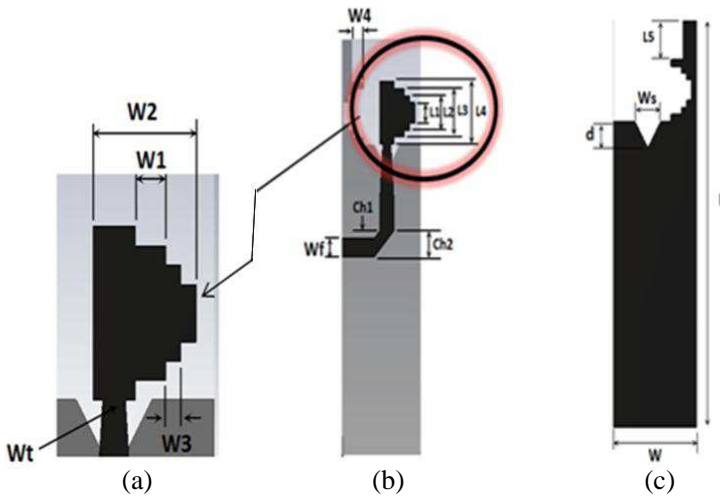


**Figure 1.** Geometry and dimensions of the proposed QSCA. (a) View of the patch, (b) top view of the proposed QSCA, and (c) back view of the proposed QSCA.

### 2.1. UWB QSCA Antenna Design

As a preliminary study and to track the effect of every modification on the performance of the antenna, a set of simulations were carried out, and the results of which are shown below. First, the case of a stepped triangular patch with a full ground plane is simulated. The results of which are shown in Figure 2. It is observed that the antenna does not fulfill the required bandwidth. For clarifying the modification process, four prototypes of the antenna are defined as follows. In Ant.1, a slot with the same shape as the patch is etched in the ground plane as mirror image (see Figure 3(a)). In Ant.2, the slot in the ground plane is rotated to face the patch (see Figure 3(b)). In Ant.3, a rectangular

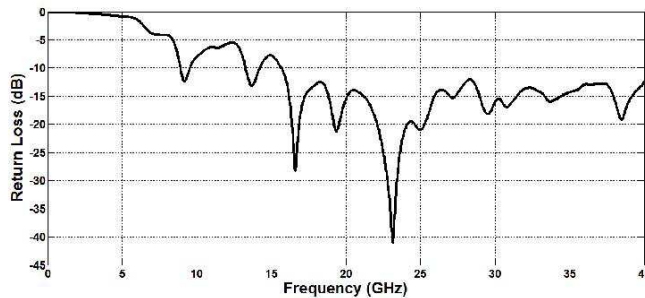


**Figure 2.** Return loss against frequency for the proposed antenna with full ground plane.

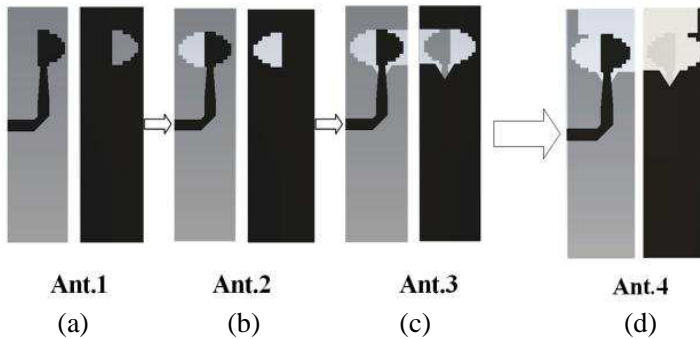


**Figure 3.** Design steps of the proposed QSCA, (a) the back slot is the same as patch and in its direction, (b) the back slot is the same as patch but rotated by 180°, (c) rectangle and triangle slots are etched in the ground plane, and (d) additional rectangular slot is etched.

slot and a triangular slot are etched in the ground plane as shown in Figure 3(c). In Ant.4, another rectangular slot is etched at the top edge of the ground plane (see Figure 3(d)).

The simulated curves of the return loss for the four antennas are plotted in Figure 4 versus frequency. For Ant.1, it is clear that the slot raises the lower limit of frequency band to a higher frequency and still without sufficient UWB performance. Also, the performance does not fulfill the required UWB characterization in Ant.2. But in Ant.3, the performance of the antenna shows UWB performance, the bandwidth which is extended from 1.5 GHz to 40 GHz with a notch around 3 GHz.

Finally, Ant.4 has fulfilled the required UWB performance of bandwidth that extends from 2.86 to more than 40 GHz as shown in Figure 4. The dimensions of the proposed QSCA antenna are obtained as the following.

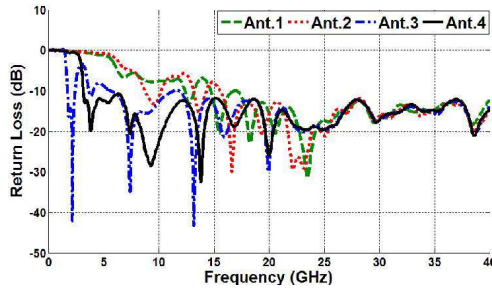


**Figure 4.** Return loss against frequency for the four antennas shown in Figure 3.

### 2.1.1. The Effect of $L$

Parametric study of  $L$  was carried out, using three different values 55, 60 and 65 mm, keeping the parameters  $L_1 = 3$  mm,  $L_2 = 5$  mm,  $L_3 = 7$  mm,  $L_4 = 9$  mm,  $L_5 = 6$  mm,  $W_1 = 2$  mm,  $W_2 = 6.8$  mm,  $W_3 = 1$  mm,  $W_4 = 2.4$  mm,  $W_s = 5$  mm,  $W_t = 1.5$  mm,  $d = 4$  mm,  $Ch_1 = 1$  mm and  $Ch_2 = 3.8$  mm, the results of which are shown in Figure 5 from which it is observed that the best value is 60 mm.

### 2.1.2. The Effect of $W_t$

The effect of the taper width  $W_t$  on the performance of the antenna is studied. The problem was first solved without implementing any tapering which moved the lower end of frequency band to 6 GHz. Results of which are shown in Figure 6, that shows the enhancement

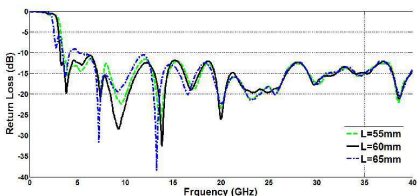


**Figure 5.** Return loss against frequency for different values of  $L$ .

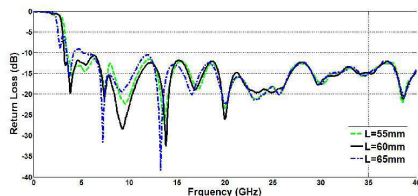


**Figure 6.** Return loss against frequency for different values of  $W_t$ .

of matching with the variation of  $W_t$ , to yield the best matching at  $W_t = 1.5$  mm. It is observed that as  $W_t$  increases more than 1.5 mm the matching deteriorates at the lower end of the frequency spectrum, whereas, as  $W_t$  decreases less than 1.5 mm the matching deteriorates around 6 GHz.

*2.1.3. The Effect of  $Ch_1$  and  $Ch_2$*

The effect of chamfering the corner of the feeding transmission line of ratio 1 : 1, for different values of  $Ch_1$  and  $Ch_2$ , are shown in Figure 7. The results show that without chamfering, the upper limit of the frequency range is lower than 7 GHz. After parametric study, it is observed that the optimum values of  $Ch_1$  and  $Ch_2$  are 1 mm, 3.8 mm, respectively.

*2.1.4. The Effect of  $d$*

Figure 8 shows the simulated return loss curves for various notch depths, ( $d = 0, 2, 4$  and 6 mm) while  $W_s = 5$  mm. When  $d = 4$  mm

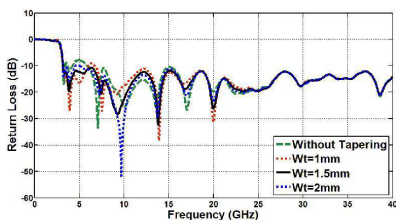


**Figure 7.** Return loss against frequency for different values of  $Ch_1$ , and  $Ch_2$ .

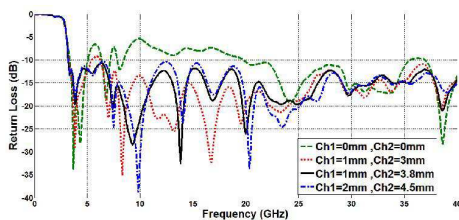


**Figure 8.** Return loss against frequency for different values of  $d$ .

the  $-10$  dB impedance bandwidth covers an ultra-wide frequency band, but when  $d$  increases to 6 mm, the impedance matching worsens around 6 GHz. Also, when  $d$  falls to 0 mm, the impedance matching of the antenna also degrades in the range from 5 to 7 GHz showing the impact of the triangular slot on the matching of the antenna.

### 2.1.5. The Effect of $W_s$

Figure 9 depicts the simulated return loss curves with different widths of the triangular notch, ( $W_s = 4, 5, 6$  and 7 mm) where  $d$  is fixed at 4 mm, It is observed from the results in Figure 9 that when  $W_s = 4$  mm, the impedance matching is not good over the entire band. When  $W_s$  increases from 4 to 7 mm the impedance matching improves then degrades again. Thus, the value of  $W_s$  does not affect the lower band behavior of the antenna, but adjusts the matching over the operational band of frequencies; the slot width is chosen to be 5 mm. The optimized values of the dimensions of the proposed antenna are listed in Table 1.

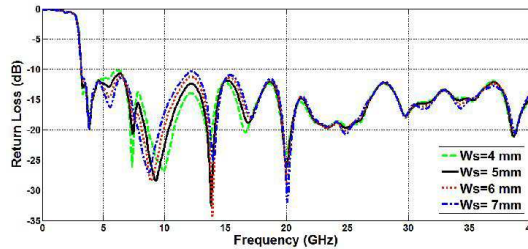


**Figure 9.** Return loss against frequency for different values of  $W_s$ .

**Table 1.** Optimized dimensions of the proposed QSCA (mm).

$L$	$L_1$	$L_2$	$L_3$	$L_4$	$L_5$	$W_1$	$W_2$	$W_3$	$W_4$	$W_s$	$W_t$	$W$	$W_f$	$d$	$ch_1$	$ch_2$
60	3	5	7	9	6	2	6.8	1	2.4	5	1.5	16	2.77	4	1	3.8

## 2.2. Band-notched UWB QSCA Antenna Design

In order to reduce the electromagnetic interference of UWB applications with the WLAN applications, a band-notched function covering the interval 5.15–5.825 GHz is recommended. To realize the proposed UWB slot antenna with band frequency notch, two U-shaped parasitic elements are placed above and below the horizontal feed line, as shown in Figure 10. The electrical length of the U-shaped parasitic



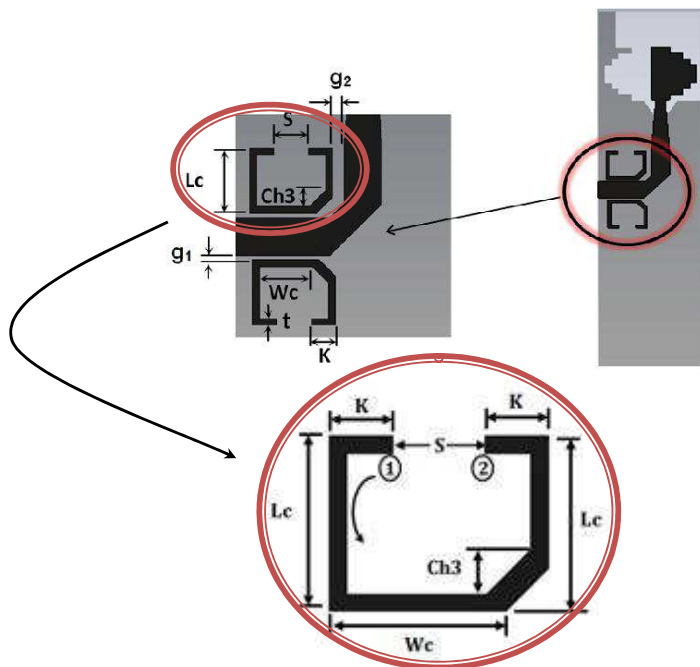


**Figure 10.** U-shaped parasitic elements for band notched frequency.

element is about  $0.5\lambda_g$  at  $f_n = 5.5$  GHz, where  $\lambda_g$  is the guided wavelength. The new created resonance frequency of the proposed antenna can be calculated as:

$$f_n = \frac{c}{2L_n\sqrt{\epsilon_{eff}}} \tag{1}$$

where,  $\epsilon_{eff} \approx (\epsilon_r + 1)/2$ , and  $L_n$  is the total length of the U-shaped parasitic elements. Adjusting the center frequency of the notch and the notch bandwidths were the challenge at this point. The total lengths of the U-shaped parasitic elements control the position of the rejected bands. Figure 11 shows the input impedance at the notch position. It was observed that any minor change in the length of the parasitic elements,  $L_n$ , has significant effect on the positions of the notch and is calculated from the inset of Figure 10 as follows:

$$L_n = 2k + 2L_c + Ch_3(\sqrt{2} - 1) + W_c \tag{2}$$

From the values obtained in Table 2, it may be concluded that the length of the U-shaped stub is governed by the approximate equation  $L_n = 0.52\lambda_{center}$ , where  $\lambda_{center}$  is the wavelength of the notch center frequency (5.5 GHz) in the substrate with dielectric constant 4.5.

**Table 2.** Optimized dimensions of the U-shaped parasitic elements.

$g_1$	$g_2$	$S$	$T$	$L_c$	$W_c$	$K$	$Ch_3$
0.3	0.8	2.5	0.5	4.8	3.8	1.75	1.2

### 3. SIMULATION AND EXPERIMENTAL RESULTS

The proposed antenna with the optimized parameters is simulated and fabricated using photolithographic technique and shown in Figure 12. Figure 13 shows the VSWR of the antenna with the two U-shaped parasitic elements, for both simulated and measured results.

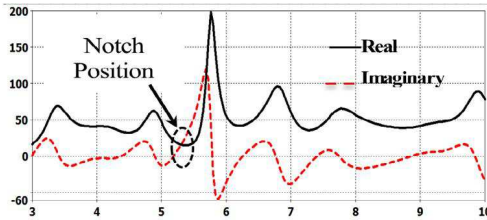
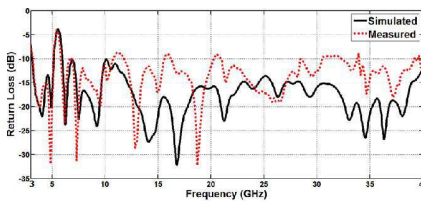


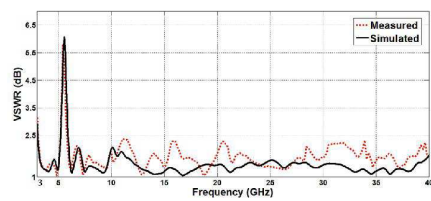
**Figure 11.** Input impedance against frequency showing the band notch.



**Figure 12.** A photo for the fabricated with two U-shaped parasitic.



(a)



(b)

**Figure 13.** Simulated and measured (a) return loss, (b) VSWR of the proposed QSCA.

### 3.1. Current Density

The simulated current density for the optimal design is displayed at 5.5 GHz and shown in Figure 14. It is observed that the current is primarily concentrated around the edges of both U-shaped parasitic elements. Therefore, its behavior acts like adding series inductance to the antenna, and a destructive interference can take place, thus, causing the antenna to be non-responsive at that frequency.

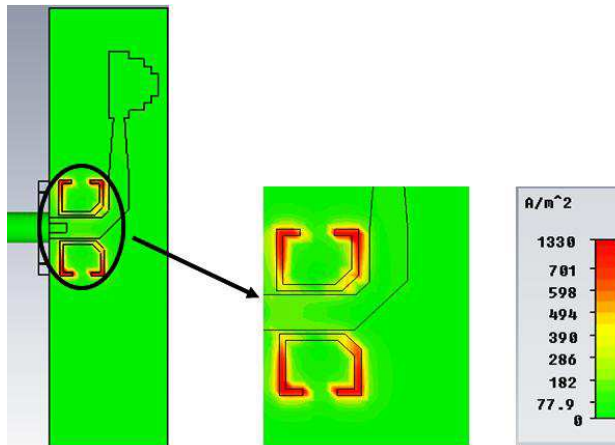


**Figure 14.** Current density at 5.5 GHz.

### 3.2. Radiation Pattern

Radiation patterns of the proposed antenna were measured using anechoic chamber model Satimo compact multi-probe antenna test station, STARLAB-18, equipped with Agilent PNA E8363B VNA,  $XZ$ -plane and  $YZ$ -plane radiation patterns. The results are shown in Figure 15 for five different frequencies, namely 3.5 GHz, 4 GHz, 7.5 GHz, 13 GHz and 17 GHz. The patterns obtained in the measurement are close to those in the simulation and relatively stable across the whole band.

## 4. PACKAGING EFFECT

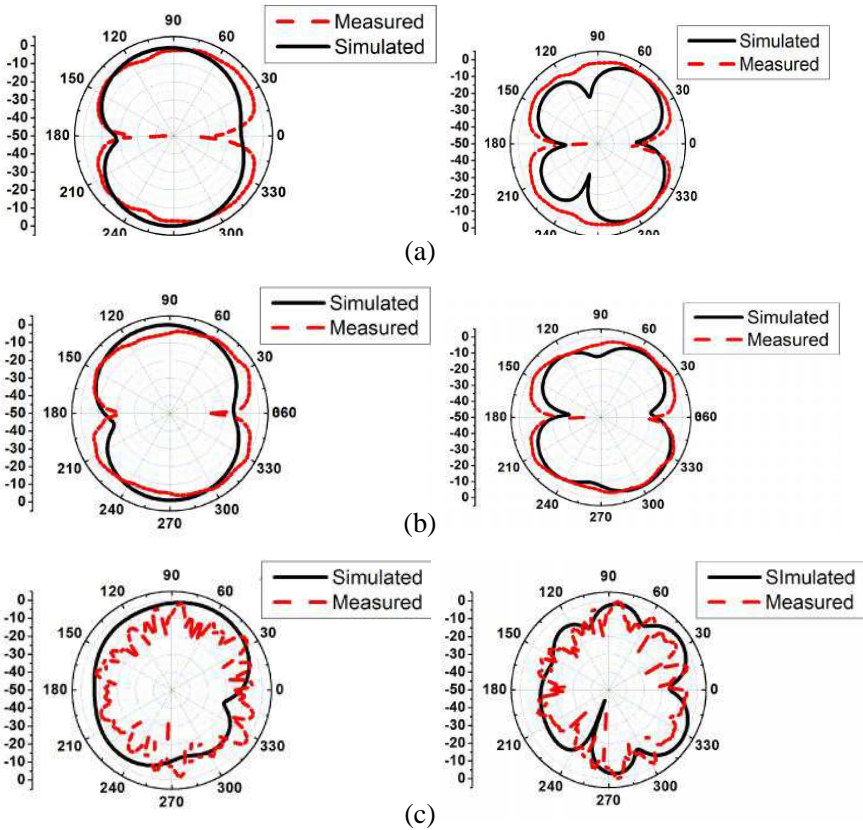
As the designed antenna is to be packaged to form an UWUSB (see Figure 16), it is worth studying the effect of this casing on the performance of the designed antenna. Two casings were considered which are available commercially, the first with  $\epsilon_r = 4.5$  and the other

with  $\epsilon_r = 2.5$ . The two casings are lossy with  $\tan \delta = 0.019$ . Figure 16 shows the antenna with the casing outlined. It is obvious that the casing is much bigger than the antenna, but the authors abide by the sizes available commercially. The SMA connector shown in Figure 16 is only included for the sake of measurements.

The return loss and VSWR of the proposed antenna are evaluated including the casing with  $\epsilon_r = 4.5$ , and  $\epsilon_r = 2.5$  and presented in Figure 17.

From Figure 17 it is observed that the performance of the proposed antenna deteriorates when the casing with  $\epsilon_r = 4.5$ , or  $\epsilon_r = 2.5$  are included in the simulation.

As using the casing is inevitable for USB applications, the design was modified to overcome the deterioration shown in Figure 17. These modifications encountered the chamfering lengths  $ch_1$  and  $ch_2$ , to enhance the matching of the antenna. After several attempts the optimum values of  $ch_1$  changed from 1 mm to 2 mm and  $ch_2$  from



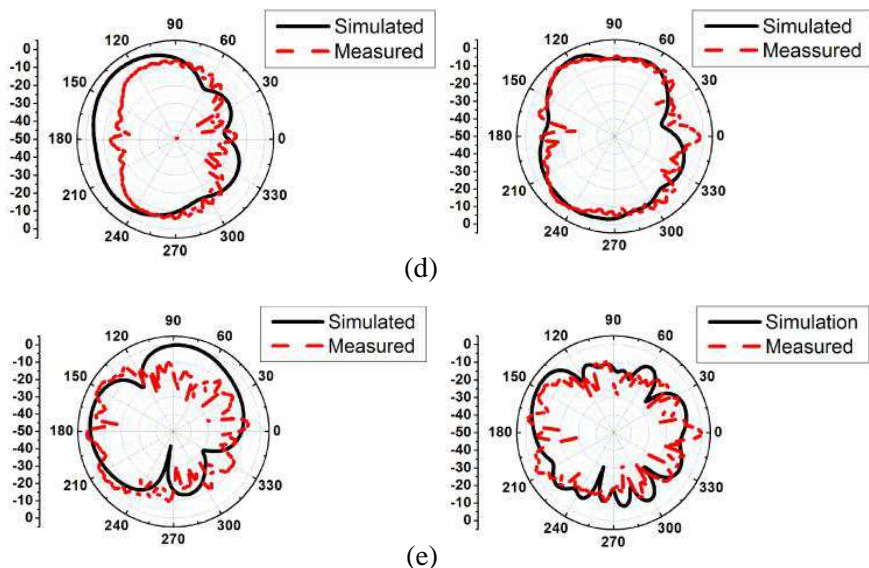


**Figure 15.** XZ- and YZ-plane radiation patterns of the proposed QSCA at (a) 3.5 GHz, (b) 4 GHz, (c) 7.5 GHz, (d) 13 GHz, and (e) 17 GHz.

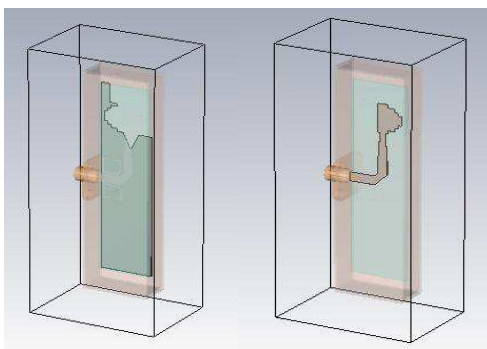


**Figure 16.** The proposed antenna with casing outlined.

3.8 mm to 3.5 mm that yielded much better performance, as shown in Figures 18(a), (b) for both  $\epsilon_r = 4.5$  and  $\epsilon_r = 2.5$ .

The gain and radiation efficiency of the antenna are shown in Figures 18(c), and (d), respectively. It is observed that the gain and radiation efficiency are stable over the whole band and have the minimum values at the notched frequency of 5.5 GHz. It is also

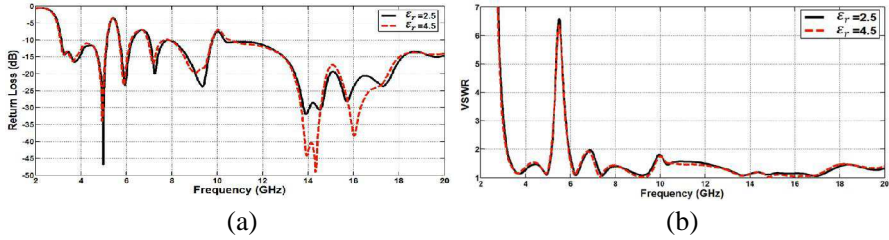


**Figure 17.** Antenna performance for  $\epsilon_r = 2.5$ , and  $\epsilon_r = 4.5$ . (a) Return loss against frequency, and (b) VSWR against frequency.

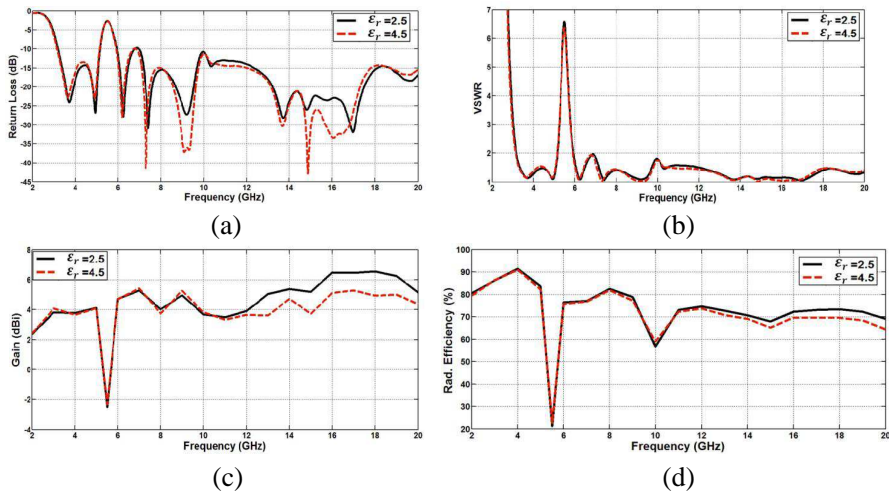


**Figure 18.** Antenna performance after optimization for  $\epsilon_r = 2.5$ , and  $\epsilon_r = 4.5$ . (a) Return loss against frequency, (b) VSWR against frequency, (c) gain against frequency, and (d) radiation efficiency against frequency.

observed that the frequency gain and radiation efficiency in the case of  $\epsilon_r = 2.5$  are better than the case of  $\epsilon_r = 4.5$ .

## 5. CONCLUSIONS

In this paper, a miniature UWB antenna for wireless USB dongle applications is presented on the basis of printed quasi-self-complementary structure fed by a microstrip line. A triangular slot is embedded in the ground plane to improve the impedance matching of the antenna. It has been illustrated that the optimal

design of this type of antennas can yield an ultra-wide impedance bandwidth with reasonable radiation properties. To accomplish such an aim, the antenna design for UWUSB dongles plays a crucial role and also presents a challenging issue because of the pace limit of the dongle boards as well as the requirements of good impedance matching and radiation property through a broad operating bandwidth. Nevertheless, to avoid interfering with nearby communication systems, such as high-performance radio local area network (HIPERLAN) (5150–5350 MHz) and WLAN (5725–5825 MHz) bands, a filter rejecting the limited band (5.15–5.825 GHz) is necessary in UWB RF front end. Instead of a filter, which complicates the system, a band-notch characteristic was introduced. This band notch was obtained using two U-shaped parasitic elements. Moreover, the antenna shows stable gain and nearly omnidirectional patterns. Therefore, the proposed antenna can be a good candidate for UWUSB applications. Finally, the design was adapted to mitigate the effects of packaging the antenna, for practical applications.

## ACKNOWLEDGMENT

This research is funded by the National Telecommunication Regulatory Authority (NTRA), Ministry of Communication and Information Technology, Egypt.

## REFERENCES

1. Uda, S. and Y. Mushiake, "Yagi-Uda antenna," Maruzen Co., Tokyo, 1954.
2. Mushiake, Y., "The input impedance of a slit antenna," *Joint Convention Record of Tohoku Sections of IEE and IECE of Japan*, 25–26, Jun. 1948.
3. Mushiake, Y., "A report on Japanese developments of antennas from Yagi-Uda antenna to self-complementary antennas," *IEEE Antennas and Propagation Society International Symposium*, Vol. 3, 841–844, 2003.
4. Ishizone, T. and Y. Mushiake, "A self-complementary antenna composed of unipole and notch antennas," *IEEE Antennas and Propagation Society International Symposium*, Vol. 15, 215–218, 1977.
5. Mushiake, Y., "Self-complimentary antennas," *IEEE Antenna and Propagation Magazine*, Vol. 34, No. 6, 23–29, Dec. 1992.

6. Mushiake, Y., "Multiterminal constant impedance antenna," *National Convention Record of IECE of Japan*, 89, Oct. 1959.
7. Mushiake, Y. and H. Saito, "Three-dimensional self-complementary antenna," *Joint Convention Record of Four Japanese Institutes Related to Electrical Engineering*, Vol. 15, No. 1212, Apr. 1963.
8. Mushiake, Y., "Constant-impedance antennas," *J. IECE Japan*, Vol. 48, No. 4, 580–584, 1965.
9. Mosallaei, H. and K. Saraband, "A compact ultra-wideband self-complementary antenna with optimal topology and substrate," *IEEE Antennas and Propagation Society International Symposium*, Vol. 2, 1859–1862, Jun. 2004.
10. MGonrdlez-Arbesu, J. and J. M. R. Romeu, "Some pre-fractal self-complementary antennas," *IEEE Antennas and Propagation Society International Symposium*, Vol. 4, 3449–3452, 2004.
11. Zhang, X., H. Guo, X. Liu, and H. Hu, "A broadband self-complementary printed antenna with axe shape," *9th International Symposium on Antennas Propagation and EM Theory (ISAPE)*, 267–270, 2010.
12. Kuroki, F., H. Ohtal, M. Yamaguchi, and E. Suematsu, "Wall-hanging type of self-complementary spiral patch antenna for indoor reception of digital terrestrial broadcasting," *IEEE International Microwave Symposium Digest*, 194–197, 2006.
13. See, T. S. P. and Z. N. Chen, "A small UWB antenna for wireless USB," *IEEE International Conference on Ultra-Wideband, (ICUWB)*, 198–203, 2007.
14. Xu, P., K. Fujimoto, and S. Lin, "Performance of quasi-self-complementary antenna using a monopole and a slot," *IEEE Antennas and Propagation Society International Symposium*, Vol. 2, 464–467, 2002.
15. Lin, C. C., C. Y. Huang, and J.-Y. Su, "Ultra-wideband quasi-self-complementary antenna with band rejection capability," *IET Microwaves, Antennas & Propagation*, Vol. 5, No. 13, 1613–1618, 2011.
16. Huang, C. Y. and J. Y. Su, "A printed band-notched UWB antenna using quasi-self-complementary structure," *IEEE Antennas and Wireless Propagation Letters*, Vol. 10, 1151–1153, 2011.
17. Kuramoto, A., "Small UWB antenna using triangular elements," *First European Conference on Antennas and Propagation, (EuCAP)*, 3715–3718, 2006.



18. Kuramoto, A., "Small UWB antenna using triangular elements on UWB unit," *First European Conference on Antennas and Propagation, (EuCAP)*, 1–4, 2006.
19. Guo, L., S. Wang, Y. Gao, Z. Wang, X. Chen, and C. G. Parini, "Study of printed quasi-self-complementary antenna for ultra-wideband systems," *Electronics Letters*, Vol. 44, No. 8, 511–512, Apr. 2008.
20. Guo, L., X. Chen, and C. G. Parini, "A printed quasi-self-complementary antenna for UWB applications," *IEEE Antennas and Propagation Society International Symposium*, 1–4, 2008.
21. Guo, L., S. Wang, Y. Gao, Z. Wang, X. Chen, and C. Parini, "A miniature quasi-self-complementary antenna for UWB applications," *Asia-Pacific Microwave Conference*, 1–4, Dec. 2008.
22. Guo, L., S. Wang, X. Chen, and C. Parini, "A small printed quasi-self-complementary antenna for ultrawide band systems," *IEEE Antennas and Wireless Propagation Letters*, Vol. 8, 554–557, 2009.
23. Guo, L., S. Wang, X. Chen, and C. Parini, "Miniature ultra-wideband antenna for wireless universal serial bus dongle applications," *IET Microwaves, Antennas & Propagation*, Vol. 6, No. 1, 113–119, 2012.